Dalton Transactions

Accepted Manuscript

ROYAL SOCIETY OF CHEMISTRY

www.rsc.org/dalton

Exceptional sensitivity to synthetic approach and halogen substituent for Zn(II) coordination assemblies with 5-halonicotinic acids

Cheng-Peng Li, Jing Chen, Yu-Hai Mu, and Miao Du*

College of Chemistry, Tianjin Key Laboratory of Structure and Performance for Functional Molecules, MOE Key Laboratory of Inorganic-Organic Hybrid Functional Material Chemistry, Tianjin Normal University, Tianjin 300387, P. R. China

* Corresponding author. *E-mail: dumiao@public.tpt.tj.cn.*

Dalton Trans.

ABSTRACT. Seven Zn(II) coordination complexes with 5-halonicotinic acids (HL-X, X = F, Cl, or Br) have been synthesized with different synthetic approaches, including layer diffusion or stirring method at ambient environment and solvothermal synthesis at 100 °C. Assembly of HL-F with Zn(II) under different conditions will yield the same 2D network of $[Zn(L\text{-}F)_2]_n$ (**1**). Interestingly, three distinct complexes, a 3D framework $\{[Zn_2(L\text{-}Cl)_4(H_2O)](H_2O)_6\}_n$ (**2**) and two 2D pseudo-polymorphic isomers $\{[Zn(L\text{-}Cl)_2](H_2O)_{1.5}\}_n$ (**3**) and $\{[Zn_2(L\text{-}Cl)_4](H_2O)\}_n$ (**4**) can be obtained by reacting HL-Cl with Zn(II) under layer diffusion, stirring, and solvothermal conditions, respectively. Further, replacing the –Cl substituent with –Br on HL-X ligand will also afford three diverse coordination assemblies of 3D $\{[Zn_2(L\text{-}Br)_4(H_2O)](CH_3OH)_{2.5}\}_n$ (**5**), mononuclear $[Zn(HL\text{-}Br)_2(H_2O)_4][L\text{-}Br]_2$ (**6**), and 2D $\{[Zn(L\text{-}Br)_2](H_2O)_{1.15}\}_n$ (**7**) depending on the synthetic pathways. Beyond the significant influence of synthetic approach, which will lead to the formation of various crystalline products, halogen substituting effect of HL-X ligands on the coordination motifs has also been demonstrated. Additionally, thermal stability and fluorescence for these crystalline materials will be presented.

Introduction

In the past decade, intensive research in the realm for crystal engineering of coordination polymers has enhanced the rational design and construction of new supramolecular architectures with diverse potential applications as optical, magnetic, catalytic, and microporous materials.[1,2] The mostly common synthetic strategy used to achieve such targeted materials is assembling the pre-designed organic ligands with specific metal ions in different solvents. In this context, the crystal growth of products can be usually performed by conventional solvent evaporation or layer diffusion approach. Notably, solvothermal synthesis has also been widely applied as a promising technique for preparing novel inorganic–organic hybrid solids, which are normally unreachable using conventional synthetic routes.[3–5] During the formation of crystalline solids in solutions by different synthetic pathways, the mechanism basically follows a liquid nucleation model, which is distinct from that for solid-state reactions (mainly involves the diffusion of atoms or ions from surface to interior of the reactants).[6]

Essentially, the structural and functional diversity for supramolecular complexes is dependent on the nature of organic or inorganic building tectons, as well as specific reaction parameters such as solvent, temperature, pH, anion, and additive etc, which have been extensively explored at this stage.[7–11] In comparison, coordination assemblies regulated by different synthetic approaches have been rarely demonstrated.[12] In our previous work, 5-halonicotinic acids (HL-X, X = F, Cl, or Br) and 5-methylnicotinic acid have been revealed to be nice candidates for different coordination assemblies, which interestingly show dynamic supramolecular response (single-crystal-to-single-crystal transformation[13]) and well-defined structural regulation by solvent,[13,14] halogen substituting effect,[14] anion[15] and so on. As a continuation of this program, we will present here a systematic study on the assembling reactions of HL-X (X = F, Cl, or Br) with Zn(II) using different synthetic routes, in order to further illustrate their influences on such coordination supramolecular systems. As a consequence, seven new complexes

with the formulas $[Zn(L\text{-}F)_2]_n$ (**1**), $\{[Zn_2(L\text{-}Cl)_4(H_2O)](H_2O)_6\}_n$ (**2**), $\{[Zn(L\text{-}Cl)_2](H_2O)_{1.5}\}_n$ (**3**), $\{[Zn_2(L\text{-}Cl)_4](H_2O)\}_n$ (**4**), $\{[Zn_2(L\text{-}Br)_4(H_2O)](CH_3OH)_{2.5}\}_n$ (**5**), $[Zn(HL\text{-}Br)_2(H_2O)_4]$- $[L\text{-}Br]_2$ (**6**), and $\{[Zn(L\text{-}Br)_2](H_2O)_{1.15}\}_n$ (**7**) were obtained under different reaction conditions, including layer diffusion, ambient stirring, and solvothermal synthesis. Remarkably, such complexes show diverse structural architectures, from the mononuclear motif to 3D coordination networks that can be well regulated by properly tuning the synthetic approaches. Thermal stability and fluorescence for these crystalline solids have also been investigated.

Experimental section

Materials and general methods

All reagents and solvents were commercially available and used as received. Elemental analyses of C, H, and N were performed on a CE-440 (Leemanlabs) analyzer. Fourier transform (FT) IR spectra (KBr pellets) were taken on an AVATAR-370 (Nicolet) spectrometer. Thermogravimetric analysis (TGA) experiments were carried out on a NETZSCH TG209 thermal analyzer in 25–700 °C temperature region at a heating rate of 10 °C/min under N_2 atmosphere. Solid state fluorescent spectra were measured on a Cary Eclipse spectrofluorimeter (Varian) at room temperature. Powder X-ray diffraction (PXRD) patterns were recorded on a Rigaku D/Max-2500 diffractometer at 40 kV and 100 mA for a Cu-target tube (λ = 1.5406 Å), with a scan speed of 2 °/min and a step size of 0.02° in 2θ. The calculated PXRD patterns were produced from the single-crystal diffraction data by using the PLATON software.[16]

Preparation of complexes 1–7

$[Zn(L\text{-}F)_2]_n$ (1).

Layer diffusion: A methanol solution (5 mL) of HL-F (28.2 mg, 0.2 mmol) was carefully layered onto a water solution (5 mL) of $Zn(NO_3)_2{\cdot}6H_2O$ (29.7 mg, 0.1 mmol) in a glass tube.

Colorless block crystals of **1** were obtained by slow evaporation of the solvent at room temperature after ten days. Yield: 22.2 mg (64%).

Stirring method: To a methanol (10 mL) solution of HL-F (28.2 mg, 0.2 mmol) was added a water solution (10 mL) of $Zn(NO_3)_2 \cdot 6H_2O$ (29.7 mg, 0.1 mmol) with continuous stirring for one hour. The mixture was filtered and then left to stand at room temperature. Colorless block crystals of **1** were obtained by slow evaporation of the solvent after three days. Yield: 22.8 mg (66%).

Solvothermal synthesis: The ligand HL-F (28.2 mg, 0.2 mmol) was dissolved in methanol (5 mL), to which a water solution (5 mL) of $Zn(NO_3)_2 \cdot 6H_2O$ (29.7 mg, 0.1 mmol) was added with stirring. The mixture was sealed in a Teflon-linear autoclave, heated at 100 °C for 5 days, and then cooled to room temperature at a rate of 10 °C/h. Colorless block crystals of **1** were obtained in 60% yield (20.7 mg).

Anal. Calcd for $C_{12}H_6ZnN_2O_4F_2$ (**1**): C, 41.71; H, 1.75; N, 8.11%. Found: C: 41.50; H, 1.71; N, 8.28%. IR (cm^{-1}): 3049m, 1619vs, 1573s, 1462s, 1437s, 1403vs, 1295m, 1254m, 1161m, 1141m, 1110m, 1028w, 956w, 933m, 824s, 790s, 693m, 620m, 456m.

$\{[Zn_2(L\text{-}Cl)_4(H_2O)](H_2O)_6\}_n$ (2). The similar layer diffusion synthetic method as that for **1** was used except that the ligand HL-F was replaced by HL-Cl (31.6 mg, 0.2 mmol). Colorless block crystals of **2** were obtained by slow evaporation of the solvent after one week in 58% yield (25.6 mg). Anal. Calcd for $C_{24}H_{26}Zn_2N_4O_{15}Cl_4$ (**2**): C, 32.64; H, 2.97; N, 6.34%. Found: C: 32.48; H, 2.85; N, 6.43%. IR (cm^{-1}): 3449b, 1631vs, 1564m, 1527w, 1426w, 1395vs, 1290m, 1237w, 1192w, 1141m, 1095w, 1030w, 912w, 872w, 789m, 748s, 687m, 584w, 454m.

$\{[Zn(L\text{-}Cl)_2](H_2O)_{1.5}\}_n$ (3). The similar ambient stirring synthetic method as that for **1** was used except that the ligand HL-F was replaced by HL-Cl (31.6 mg, 0.2 mmol). Colorless block crystals of **3** were obtained by slow evaporation of the solvent after four days. Yield: 25.4 mg

(63%). Anal. Calcd for $C_{12}H_9ZnN_2O_{5.5}Cl_2$ (**3**): C, 35.54; H, 2.24; N, 6.91%. Found: C: 35.77; H, 2.10; N, 7.07%. IR (cm^{-1}): 3564b, 1615vs, 1560s, 1447s, 1394vs, 1297m, 1243w, 1189w, 1129m, 1107m, 1031m, 923m, 905m, 778vs, 688m, 556w, 460m.

$\{[Zn_2(L\text{-}Cl)_4](H_2O)\}_n$ (4). The similar solvothermal synthesis as that for **1** was used except that the ligand HL-F was replaced by HL-Cl (31.6 mg, 0.2 mmol). Colorless block crystals of **4** were obtained in 62% yield (24.1 mg). Anal. Calcd for $C_{24}H_{14}Zn_2N_4O_9Cl_4$ (**4**): C, 37.20; H, 1.82; N, 7.23%. Found: C: 37.05; H, 1.79; N, 7.36%. IR (cm^{-1}): 3424b, 1634s, 1602vs, 1554m, 1402m, 1358vs, 1366m, 1332w, 1221w, 1162w, 1103w, 1066w, 977m, 939m, 832s, 732s, 701m, 662w, 607m, 511m.

$\{[Zn_2(L\text{-}Br)_4(H_2O)](CH_3OH)_{2.5}\}_n$ (5). The similar layer diffusion synthetic method as that for **1** was used except that the ligand HL-F was replaced by HL-Br (40.4 mg, 0.2 mmol). Colorless block crystals of **5** were obtained by slow evaporation of the solvent after ten days in 50% yield (26.0 mg). Anal. Calcd for $C_{26.5}H_{24}Zn_2N_4O_{11.5}Br_4$ (**5**): C, 30.82; H, 2.34; N, 5.42%. Found: C: 30.67; H, 2.30; N, 5.57%. IR (cm^{-1}): 3433b, 1636vs, 1556m, 1388vs, 1291m, 1092s, 1026s, 871w, 786m, 740w, 687m, 620w, 533m, 453w.

$[Zn(HL\text{-}Br)_2(H_2O)_4][L\text{-}Br]_2$ (6). The similar ambient stirring synthetic method as that for **1** was used except that the ligand HL-F was replaced by HL-Br (40.4 mg, 0.2 mmol). Colorless block crystals of **6** were obtained by slow evaporation of the solvent after six days in 54% yield (25.3 mg, based on HL-Br). Anal. Calcd for $C_{24}H_{22}ZnN_4O_{12}Br_4$ (**6**): C, 30.55; H, 2.35; N, 5.94%. Found: C: 30.41; H, 2.28; N, 6.07%. IR (cm^{-1}): 3410b, 3077s, 1720s, 1619vs, 1560m, 1443w, 1378vs, 1317m, 1292vs, 1178w, 1128m, 1088m, 1029w, 916w, 856w, 794m, 768m, 720m, 686m, 543w.

$\{[Zn(L\text{-}Br)_2](H_2O)_{1.15}\}_n$ (7). The similar solvothermal synthesis as that for **1** was used except that the ligand HL-F was replaced by HL-Br (40.4 mg, 0.2 mmol), producing colorless block crystals of **7** in 55% yield (26.9 mg). Anal. Calcd for $C_{12}H_{8.3}ZnN_2O_{5.15}Br_2$ (**7**): C, 29.53; H,

1.71; N, 5.74%. Found: C: 29.83; H, 1.52; N, 5.94%. IR (cm^{-1}): 3434b, 1623vs, 1583w, 1558w, 1441w, 1386s, 1329m, 1293m, 1113m, 1086m, 917w, 854w, 788w, 765w, 721w, 687m, 534w.

X-ray crystallography

Single-crystal X-ray diffraction data for **1**–**7** (CCDC: 1001894 and 1001896–1001901) were collected on a Bruker Apex II CCD diffractometer with Mo Kα radiation (λ = 0.71073 Å, for **1** and **3**–**7**) or Cu Kα radiation (λ = 1.54178 Å, for **2**) at ambient temperature (for **1**–**3** and **6**–**7**) or 173(2) K (for **4** and **5**). For each sample, a semi-empirical absorption correction was applied (SADABS) and the program SAINT was used for integration of the diffraction profiles.[17] All structures were solved by direct methods (SHELXS) and refined with SHELXL.[18] The final refinements were completed by full-matrix least-squares methods with anisotropic thermal parameters for all non-H atoms on F^2. Generally, C-bound H atoms were geometrically placed and refined as riding, whereas O-bound H atoms were first determined in difference Fourier maps and then fixed in the calculated positions. Isotropic displacement parameters of H atoms were derived from the parent atoms. The lattice solvents in **2** and **5** were treated as the diffuse contribution to the overall scattering without specific atom sites by SQUEEZE/PLATON. In addition, the lattice water molecules of O6 (in **3**), O3 (in **4**), and O5/O6 (in **7**) were assigned to 0.25, 0.25, and 0.80/0.35 occupancy, respectively, to achieve the appropriate thermal parameters. The affiliated hydrogen atoms of O6 in **7** cannot be located. Notably, single crystals for **7** with good quality were not obtained after several attempts (see Scheme 2 for crystal photo), resulting in the rather poor diffraction data. Further crystallographic details are given in Table S1 and selected bond parameters are listed in Table S2 (see ESI†).

Results and discussion

Synthesis and general characterization

Three different synthetic approaches (layer diffusion, ambient stirring, and solvothermal synthesis) were applied for the assembled systems of $Zn(NO_3)_2$ and HL-X in H_2O–CH_3OH to afford complexes **1**–**7** (Scheme 1). The Zn(II)/HL-F system is independent to the synthetic conditions. However, for the Zn(II)/HL-Cl or Zn(II)/HL-Br system, the three synthetic routes will lead to the formation of completely different complexes **2**–**4** or **5**–**7**. In fact, such a systematic regulation on the construction of diverse coordination assemblies via controlling the synthetic approach is extremely unusual.[12] All crystalline products were characterized by IR, elemental analysis, and single crystal X-ray diffraction, the phase purity of which was further confirmed by PXRD patterns (Fig. S1, ESI†). In IR spectra of **2**–**7**, the broad peaks centered at *ca.* 3400 cm^{-1} indicate the O–H characteristic stretching vibrations of water, methanol, and/or carboxyl. The IR spectrum of **6** shows a strong absorption peak at 1720 cm^{-1}, revealing the presence of –COOH group of HL-Br. In contrast, the absence of characteristic absorption band of carboxyl (*ca.* 1700 cm^{-1}) in IR spectra of **1**–**5** and **7** confirms a complete deprotonation of the HL-X ligands. As a result, the antisymmetric and symmetric stretching vibrations of the carboxylate groups appear in the range of 1602–1636 and 1358–1403 cm^{-1}, respectively.

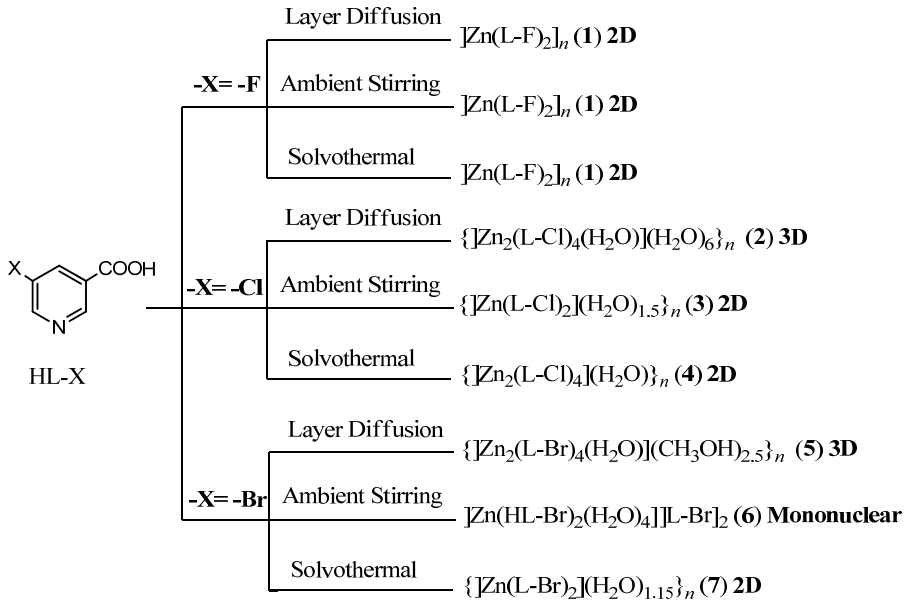

Scheme 1 Synthetic approaches for Zn(II) complexes with 5-halonicotinic acids.

Structural description of 1–7

$[Zn(L\text{-}F)_2]_n$ (1). Complex **1** crystallizes in the orthorhombic system with *Fdd*2 space group. The asymmetric unit comprises one half-occupied Zn(II) ion and one L-F^- ligand (see Fig. 1a). Each Zn(II) ion adopts a distorted octahedral geometry, provided by four carboxylate O atoms and two pyridyl N donors coming from four different L-F^- ligands. The Zn–O bond distances are in the range of 2.0168(19)–2.401(2) Å, while the Zn–N bond length is 2.099(2) Å. The bond angles around the Zn(II) center are in the range of 58.95(8)–153.71(7)°. Each L-F^- ligand acts as a μ_2-bridge with one pyridyl plus one chelating carboxylate groups (see Chart 1a), extending the adjacent Zn(II) ions to form a 2D (4,4) layer along the *ac* plane (Fig. 1b). Each rhombus $[Zn_4(L\text{-}F)_4]$ repeating unit has a side length of 7.792(1) Å, the internal angles of 76.2(1) and 103.8(1)°, and the diagonal Zn···Zn distances of 9.612(2) and 12.266(2) Å. These parallel 2D layers stack in an interdigitating mode along the [010] axis (Fig. 1c).

(Insert **Fig. 1** here)

$\{[Zn_2(L\text{-}Cl)_4(H_2O)](H_2O)_6\}_n$ (2). In the 3D coordination polymer **2**, the asymmetric coordination unit comprises one Zn(II) center, two crystallographically independent L-Cl^- ligands, and a half-occupied water ligand (Fig. 2a). Each Zn(II) ion is six-coordinated to four O atoms from three carboxylates and one water, and two N donors from two pyridyl groups, forming a distorted octahedral geometry. The Zn–O bond distances are in the range of 2.087(2)–2.192(2) Å, while the Zn–N bond lengths are 2.140(2) and 2.184(2) Å. The bond angles around Zn(II) are in the range of 83.37(9)–175.30(9)°. Two adjacent Zn(II) ions are triply bridged by two carboxylates and one water to form a $[Zn_2(H_2O)(COO)_2]$ SBU, with the Zn···Zn separation of 3.547(1) Å. Two types of L-Cl^- ligands play the μ_2- and μ_3-bridging roles, respectively (Chart 1b and 1c), which extend such dimeric motifs to construct a 3D polymeric framework (see Fig. 2b, left). Notably, the μ_2- and μ_3-L-Cl^- ligands connect the Zn(II) ions to afford two different 1D arrays along the [100] and [001] directions, respectively (see Fig. 2b, right). This structure

contains 1D channels along the [001] direction, with the solvent-accessible voids of 696.6 $Å^3$ (21.9% per unit cell unit) as calculated by PLATON. From the viewpoint of net topology, the Zn(II) ions and μ_3-L-Cl^- ligands act as the 6- and 3-connected nodes, with μ_2-L-Cl^- ligands as the 2-connected linkers. Thus, the 3D structure can be classified to a binodal (3,6)-connected framework with the point symbol of $(3.4.5)(3^2.4^3.5^3.6.7^4.8^2)$ (see Fig. 2c). Alternatively, each $[Zn_2(H_2O)(COO)_2]$ SBU can also be regarded as a node that is connected to four nearby SBUs through the L-Cl^- ligands, leading to a uninodal 4-connected **dia** network (see Fig. 2d).[19]

(Insert **Fig. 2** here)

$\{[Zn(L\text{-}Cl)_2](H_2O)_{1.5}\}_n$ (3). The asymmetric coordination unit of **3** consists of one Zn(II) center and two crystallographically independent L-Cl^- ligands (Fig. 3a). Each Zn(II) takes an octahedral geometry that is surrounded by four O atoms of two carboxylates and two nitrogen atoms of pyridyl rings, coming from four different L-Cl^- ligands. The Zn–O bond lengths are in the range of 2.027(2)–2.361(3) Å, whereas the Zn–N bond lengths are 2.071(2) and 2.078(2) Å. The bond angles around Zn(II) ions are in the range of 58.51(9)–153.68(9)°. The L-Cl^- ligands bridge the Zn(II) centers (Chart 1d) to afford a 2D layered network along the *ab* plane (see Fig. 3b), in which the repeating square $[Zn_4(L\text{-}Cl)_4]$ units are arranged in an edge-sharing fashion, with the side and diagonal Zn···Zn distances of 7.716(1)/7.740(1) Å and 10.929(1) Å, respectively. The paired layers are arranged in an interdigitating fashion to facilitate π–π interactions between the parallel pyridyl rings with the centroid-to-centroid separation of 3.684(2) Å. Additionally, hydrogen-bonding interaction between the carboxylates of paired layers and the lattice water (H–O and O···O = 2.07 Å and 2.844 Å, O–H···O = 151°) as well as those between the lattice water molecules (H–O and O···O = 2.12–2.35 Å and 2.851 Å, O–H···O = 118–144°) are observed, which lead to the formation of a 3D supramolecular network (see Fig. 3c).

(Insert **Fig. 3** here)

{[Zn_2(L-Cl)$_4$](H$_2$O)}$_n$ (4). The asymmetric coordination unit of complex **4** consists of one half-occupied Zn(II) ion and one crystallographically independent L-Cl$^-$ ligand (see Fig. 4a). Each Zn(II) center adopts the distorted octahedral geometry with the contribution from four O atoms of two carboxylates and two pyridyl N donors coming from four different L-Cl$^-$ ligands. The Zn–O bond distances are in the range of 2.041(5)–2.351(5) Å and the Zn–N bond length is 2.099(4) Å. The bond angles around the Zn(II) ion are in the range of 59.33(19)–156.1(3)°. Similar to those in **1** and **3**, the Zn(II) centers are extended by the L-Cl$^-$ linkers (see Chart 1d) to afford a 2D polymeric layer along the *ab* plane (see Fig. 4b). Again, the repeating rhombic [Zn_4(L-Cl)$_4$] units are observed, in which the side and diagonal Zn···Zn distances are 7.786(1) and 9.822(1)/12.084(1) Å and the internal angles are 101.79(1) and 78.21(1)°. Also, the adjacent layers are closely packed in an interdigitating mode, in which aromatic stacking interactions between the parallel pyridyl groups are found to further stabilize the 3D supramolecular network, with the centroid-to-centroid separation of 3.542(2) Å (see Fig. 4c).

(Insert **Fig. 4** here)

[Zn(HL-Br)$_2$(H$_2$O)$_4$][L-Br]$_2$ (6). In the asymmetric unit of the ion-paired complex **6**, there exist two crystallographically independent Zn(II) ions with half occupancy, two coordinative HL-Br ligands, four water ligands, and two isolated L-Br$^-$ anions (see Fig. 5a). Both Zn1 and Zn2 similarly take the six-coordinated octahedral geometries, which are surrounded by four O atoms from four water molecules and two N donors from a pair of HL-Br ligands (see Chart 1f). The Zn–O bond distances are in the range of 2.046(3)–2.111(3) Å, while the Zn–N bond lengths are 2.176(3) and 2.239(3) Å. The bond angles around the Zn(II) center are in the range of 88.07(12)–180.0°. The carboxyl groups of HL-Br ligand are hydrogen bonded to the uncoordinated pyridyl rings of L-Br$^-$ (O2–H2···N3: H···N and O···N = 1.80 and 2.615(5) Å, O–H···N = 176°; O3–H3···N4^i: H···N and O···N = 1.82 and 2.642(5) Å, O–H···N = 176°, i = 1 – *x*, *y*, 1/2 – *z*). Further, the water ligands are linked to the carboxylate of L-Br$^-$ or carboxyl of

HL-Br via multiple O–H···O H-bonding (H···O and O···O = 1.81–2.01 and 2.672(5)–2.782(5) Å, O–H···O = 149–173°) to form a 2D supramolecular network (Fig. 5b). In addition, intra-layer aromatic stacking interactions occur between the pyridyl groups of L-Br$^-$, with the centroid-to-centroid distances of 3.540(3)–3.683(3) Å and dihedral angles of 0.93–1.63°. No significant interaction is found between these 2D layers.

(Insert **Fig. 5** here)

$\{[Zn_2(L\text{-}Br)_4(H_2O)](CH_3OH)_{2.5}\}_n$ (5) and $\{[Zn(L\text{-}Br)_2](H_2O)_{1.15}\}_n$ (7). Complexes **5** and **7** are isostructural to complexes **2** and **3**, respectively, and their structures will not be discussed.

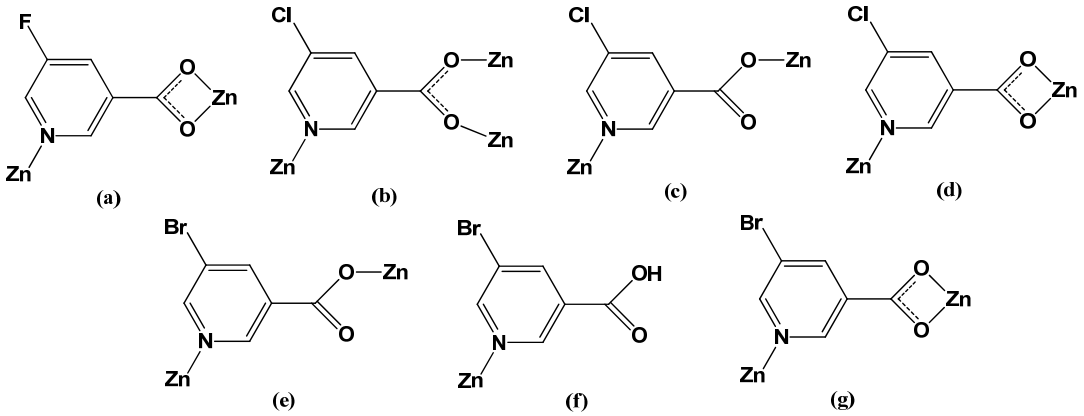

Chart 1 Coordination modes of HL-X ligands in this work: (a) for **1**; (b) and (c) for **2**; (d) for **3** and **4**; (e) and (f) for **5**; (g) for **6**; (h) for **7**.

Effect of reaction conditions and halogen substituents on structural assembly

This work aims to illustrate the influence of different reaction conditions and ligand halogen substituents on the formation of diverse crystalline supramolecular complexes (see Scheme 2). As a role, layer diffusion method allows the slowest reaction rate with different local concentrations of reactants, ambient stirring facilitates a full mixing of the reactants under mild condition, while solvothermal synthesis can provide the most drastic reaction environment under higher temperature and pressure in a closed vessel. Nevertheless, only modifying the synthetic

method, with other reaction parameters keeping constant, is actually difficult to yield different products, especially in the forms of high-quality single crystals for X-ray diffraction analysis. Herein, the coordination assembled systems of Zn(II) with HL-Cl or HL-Br show exceptional sensitivity to synthetic approaches, resulting in a variety of 2D and 3D coordination polymers and a charge-assistant H-bonding supramolecular complex, which however is not observed in the case of HL-F. Of particular interest, all crystalline products under solvothermal synthesis possess the 2D layered networks (HL-F for **1**, HL-Cl for **4**, and HL-Br for **7**), while different 3D lattices are constructed relying on the secondary interactions (none for **1**, aromatic stacking for **4**, and H-bonding/aromatic stacking for **7**). Notably, **3** and **4** with 2D square or rhombic (4,4) layers are a pair of pseudo-polymorphic isomers.

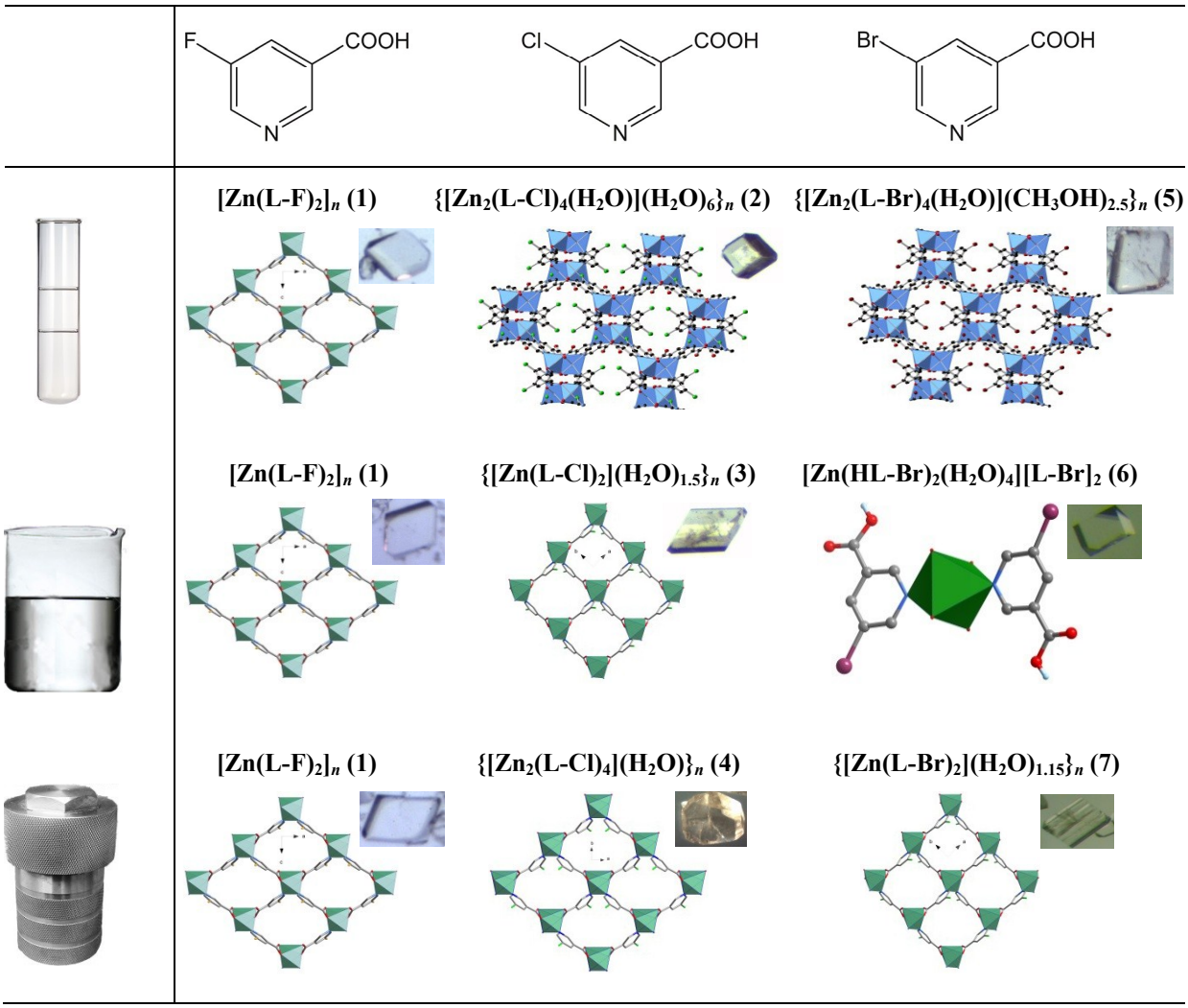

Scheme 2 Comparison of the coordination assemblies of Zn(II) with 5-halonicotinic acids.

On the other hand, the significant halogen substituent effect on the construction of different structures is also observed in these assembled systems. In fact, the substituted halogen groups of –F, –Cl, and –Br with distinct electronegativity, polarizability, and steric accessibility may heavily modulate the resulting coordination architectures. For example, using the similar layer diffusion approach, assemblies of HL-X with Zn(II) afford the 2D layer of **1**, and isostructural 3D networks of **2** and **5**, respectively. For ambient stirring route, it is of great significance that three different coordination assemblies with 2D layers of **1** and **3**, and a mononuclear pattern of **6** are obtained, by changing the halogen substituents of the ligands. In this regard, it may be deduced that the coordination ability for 5-halonicotinic acids will be in a decreasing order of HL-F > HL-Cl > HL-Br, which corresponds to the electronegativity trend and the strength of electron-withdrawing effect of halogens (–F > –Cl > –Br). As a result, only the L-F^- ligand is observed in the final products, while for the assembled systems with L-Cl^- and L-Br^-, the water molecules may also be involved in metal coordination, which will promote their structural diversity. Notably, although these coordination assemblies can be well modulated by the reaction approaches and halogen substituents, the inherent mechanism is still not clear and hard to be specified at this stage. Actually, the Cd(II) assembled systems with such HL-X ligands also show significant crystallization diversity, which however are primarily directed by the solvent effect.[13a,14] In comparison, assembly of HL-F with Zn(II) or Cd(II) will afford single or three[14] products, which show 2D layer or 2D/3D structures with different ligand coordination modes (see Charts 1 and S1). Similar case is also found for M^{IIB}/HL-Cl system, where three or four[14] 2D/3D coordination networks are achieved. Significantly, more diversity can be observed for M^{IIB}/HL-Br system in terms of both ligand binding fashions and final products, in which three Zn(II) complexes with 0D/2D/3D motifs and as many as nine Cd(II) coordination polymers[13a] ranging from 1D to 3D are directed by synthetic approaches and solvents, respectively.

Thermal stability

All complexes **1**–**7** are air stable and their thermal stability was explored by TGA experiments (see Fig. S2). Complex **1** is stable to 340 °C, followed by a sharp weight loss that will not stop until heating to 700 °C. The TGA curve for **2** shows two continuous weight losses of 13.31% in the region of 48–215 °C, corresponding to the removal of six lattice water molecules (calculated: 12.23%). The residual sample starts to decompose at 335 °C, with a sharp weight loss that does not end until heating to 700 °C. For **3**, the first weight loss of 5.47% in the range of 30–113 °C reveals the exclusion of all lattice water molecules (calculated: 6.66%). Pyrolysis of the residual host framework occurs at 337 °C, with a sharp weight loss that will not stop until heating to 700 °C. The TGA curve of **4** displays the first weight loss of 2.11% in 25–150 °C, indicating the exclusion of one lattice water (calculated: 2.32%). The host framework will be thermally stable to 300 °C and then suffers a sharp weight loss that does not stop until heating to 700 °C. Similar to that of **2**, the TGA curve for **5** exhibits two continuous weight losses of 7.75% in 30–224 °C, corresponding to the exclusion of lattice methanol molecules (calculated: 7.74%). Pyrolysis of the host framework is observed at 342 °C with a sharp weight loss which does not stop until heating to 700 °C. For **6**, the first weight loss of 6.90% (calculated: 7.63%) in 38–122 °C corresponds to the exclusion of four coordinated water molecules. Then, a sharp weight loss of 41.83% is found in 160–257 °C, revealing the loss of two lattice HL-Br molecules (calculated: 42.82%). The residual solid is thermally stable to 370 °C, with that, a series of continuous weight losses are observed, which do not stop until the heating end. Complex **7** shows the first weight loss of 3.26% in 30–115 °C, revealing the removal of all lattice water molecules (calculated: 4.24%). Pyrolysis of the host coordination network occurs at 325 °C, with a sharp weight loss that does not end until heating to 700 °C.

Photoluminescence properties

Polymeric complexes with d^{10} metal centers such as Zn(II) and conjugated organic ligands are promising candidates for photoactive crystalline materials with potential applications.[20] Thus, solid-state fluorescent spectra for HL-X ligands and complexes **1**–**7** (see Fig. 6) were recorded at room temperature (λ_{ex} = 336 nm). The emission spectra of HL-F, HL-Cl, and HL-Br exhibit the similar profiles with the maximal peaking at 496 nm. Excitation of the crystalline samples for complexes **1**–**7** at 336 nm leads to the generation of similar fluorescent emissions with the peak maxima at 495–497 nm, which reveals a ligand-based mechanism for their luminescence. Moreover, the enhancement of emission intensity for **1**–**7** compared with those of the corresponding ligands can be attributed to the increased rigidity of HL-X when bound to the Zn(II) center, which effectively reduces the loss of energy.

(Insert **Fig. 6** here)

Conclusions and perspective

In summary, we have systematically investigated the effect of synthetic approach and halogen substituent on coordination assemblies of Zn(II) with 5-halonicotinic acids. Significantly, this work provides a series of peculiar prototypes to illustrate the critical regulating factor for such supramolecular complexes. The results urge us to further explore the subtle modulation of related coordination systems, involving nicotinic acids with different substituents (–CH_3, –NO_2, –OH, or –NH_2) and other metal centers (Ag^I, Cu^{II}, Pb^{II}, or Ln^{III}) with adaptable coordination geometries, which will be helpful to understand their intrinsic assembled mechanisms and to construct new crystalline materials with desired structures and properties.

Acknowledgments

This work was supported by the National Natural Science Foundation of China (21031002 and 21101116), Program for Innovative Research Team in University of Tianjin (TD12-5038), and Innovation Foundation of Tianjin Normal University (52XC1402).

Electronic Supplementary Information (ESI) available: Tables for crystallographic parameters and selected bond lengths and angles, Chart for ligand coordination modes, powder X-ray diffraction (PXRD) patterns, and thermogravimetric analysis (TGA) curves. For ESI and crystallographic data in CIF or other electronic format see DOI: 10.1039/b000000x/

References

(1) (*a*) S. L. Li and Q. Xu, *Energy Environ. Sci.*, 2013, **6**, 1656; (*b*) J. R. Li, J. Sculley and H. C. Zhou, *Chem. Rev.*, 2012, **112**, 869; (*c*) M. Du, C. P. Li, C. S. Liu and S. M. Fang, *Coord. Chem. Rev.*, 2013, **257**, 1282; (*d*) J. Gascon, A. Corma, F. Kapteijn and F. X. L. I. Xamena, *ACS Catal.*, 2014, **4**, 361; (*e*) G. P. Yang, L. Hou, X. J. Luan, B. Wu and Y. Y. Wang, *Chem. Soc. Rev.*, 2012, **41**, 6992; (*f*) Y. J. Cui, Y. F. Yue, G. D. Qian and B. L. Chen, *Chem. Rev.*, 2012, **112**, 1126; (*g*) E. Coronado and G. M. Espallargas, *Chem. Soc. Rev.*, 2013, **42**, 1525.

(2) (*a*) M. M. Wanderley, C. Wang, C. D. Wu and W. B. Lin, *J. Am. Chem. Soc.*, 2012, **134**, 9050; (*b*) H. L. Jiang, D. W. Feng, K. C. Wang, Z. Y. Gu, Z. W. Wei, Y. P. Chen and H. C. Zhou, *J. Am. Chem. Soc.*, 2013, **135**, 13934; (*c*) F. J. Song, C. Wang and W. B. Lin, *Chem. Commun.*, 2011, **47**, 8256; (*d*) C. E. Wilmer, M. Leaf, C. Y. Lee, O. K. Farha, B. G. Hauser, J. T. Hupp and R. Q. Snurr, *Nat. Chem.*, 2012, **4**, 83; (*e*) B. Gole, A. K. Bar, A. Mallick, R. Banerjee and P. S. Mukherjee, *Chem. Commun.*, 2013, **49**, 7439; (*f*) P. Nugent, Y. Belmabkhout, S. D. Burd, A. J. Cairns, R. Luebke, K. Forrest, T. Pham, S. Q. Ma, B. Space, L. Wojtas, M. Eddaoudi and M. J. Zaworotko, *Nature*, 2013, **495**, 80; (*g*) Z. J. Zhang, L. Wojtas, M. Eddaoudi and M. J. Zaworotko, *J. Am. Chem. Soc.*, 2013, **135**, 5982.

(3) (*a*) X. M. Chen and M. L. Tong, *Acc. Chem. Res.*, 2007, **40**, 162; (*b*) X. M. Zhang, *Coord. Chem. Rev.*, 2005, **249**, 1201; (*c*) S. H. Feng and R. R. Xu, *Acc. Chem. Res.*, 2001, **34**, 239; (*d*) J. Y. Lu, *Coord. Chem. Rev.*, 2003, **246**, 327.

(4) (*a*) J. P. Zhang, S. L. Zheng, X. C. Huang and X. M. Chen, *Angew. Chem. Int. Ed.*, 2004, **43**, 206; (*b*) J. Tao, Y. Zhang, M. L. Tong, X. M. Chen, T. Yuen, C. L. Lin, X. Y.

Huang and J. Li, *Chem. Commun.*, 2002, 1342; (*c*) C. M. Liu, S. Gao and H. Z. Kou, *Chem. Commun.*, 2001, 1670; (*d*) H. Zhao, Z. R. Ou, H. Y. Ye and R. G. Xiong, *Chem. Soc. Rev.*, 2008, **37**, 84; (*e*) C. P. Li, X. H. Zhao, X. D. Chen, Q. Yu and M. Du, *Cryst. Growth Des.*, 2010, **10**, 5034.

(5) R. M. Barrer, *Hydrothermal Chemistry of Zeolites*; Academic Press: London, 1982.

(6) (*a*) J. J. Vittal, *Coord. Chem. Rev.*, 2007, **251**, 1781; (*b*) M. Kawano and M. Fujita, *Coord. Chem. Rev.*, 2007, **251**, 2592; (*c*) J. Marti-Rujas, Y. Matsushita, F. Izumi, M. Fujita and M. Kawano, *Chem. Commun.*, 2010, **46**, 6515.

(7) (*a*) F. A. A. Paz, J. Klinowski, S. M. F. Vilela, J. P. C. Tome, J. A. S. Cavaleiro and J. Rocha, *Chem. Soc. Rev.*, 2012, **41**, 1088; (*b*) J. H. Fu, H. J. Li, Y. J. Mu, H. W. Hou and Y. T. Fan, *Chem. Commun.*, 2011, **47**, 5271; (*c*) L. Hou, W. J. Shi, Y. Y. Wang, Y. Guo, C. Jin and Q. Z. Shi, *Chem. Commun.*, 2011, **47**, 5464; (*d*) V. Colombo, C. Montoro, A. Maspero, G. Palmisano, N. Masciocchi, S. Galli, E. Barea and J. A. R. Navarro, *J. Am. Chem. Soc.*, 2012, **134**, 12830; (*e*) C. Hou, Q. Liu, J. Fan, Y. Zhao, P. Wang and W. Y. Sun, *Inorg. Chem.*, 2012, **51**, 8402.

(8) (*a*) C. Li, D. S. Li, J. Zhao, Y. Q. Mou, K. Zou, S. Z. Xiao and M. Du, *CrystEngComm*, 2011, **13**, 6601; (*b*) C. P. Li and M. Du, *Inorg. Chem. Commun.*, 2011, **14**, 502; (*c*) M. Du, C. P. Li and J. H. Guo, *CrystEngComm*, 2009, **11**, 1536; (*d*) Z. J. Lin, T. F. Liu, Y. B. Huang, J. Lu and R. Cao, *Chem.–Eur. J.*, 2012, **18**, 7896; (*e*) H. Wang, Z. Chang, Y. Li, R. M. Wen and X. H. Bu, *Chem. Commun.*, 2013, **49**, 6659; (*f*) A. J. Calahorro, M. E. López-Viseras, A. Salinas-Castillo, D. Fairen-Jimenez, E. Colacio, J. Cano and A. Rodríguez-Diéguez, *CrystEngComm*, 2012, **14**, 6390.

(9) (*a*) C. P. Li and M. Du, *Chem. Commun.*, 2011, **47**, 5958; (*b*) H. Wang, Y. Y. Wang, G. P. Yang, C. J. Wang, G. L. Wen, Q. Z. Shi and S. R. Batten, *CrystEngComm*, 2008, **10**, 1583; (*c*) F. Yuan, J. Xie, H. M. Hu, C. M. Yuan, B. Xu, M. L. Yang, F. X. Dong and G. L. Xue, *CrystEngComm*, 2013, **15**, 1460; (*d*) X. Bao, H. J. Shepherd, L. Salmon, G. Molnar, M. L. Tong and A. Bousseksou, *Angew. Chem. Int. Ed.*, 2013, **52**, 1198; (*e*) Y. W. Li, K. H. He and X. H. Bu, *J. Mater. Chem. A*, 2013, **1**, 4186.

(10) (*a*) L. M. Fan, X. T. Zhang, D. C. Li, D. Sun, W. Zhang and J. M. Dou, *CrystEngComm*,

2013, **15**, 349; (*b*) D. F. Sun, S. Q. Ma, J. M. Simmons, J. R. Li, D. Q. Yuan and H. C. Zhou, *Chem. Commun.*, 2010, **46**, 1329; (*c*) Y. C. Ou, D. S. Zhi, W. T. Liu, Z. P. Ni and M. L. Tong, *Chem.–Eur. J.*, 2012, **18**, 7357; (*d*) Q. Liu, L. N. Jin and W. Y. Sun, *Chem. Commun.*, 2012, **48**, 8814.

(11) (*a*) W. W. Dong, D. S. Li, J. Zhao, L. F. Ma, Y. P. Wu and Y. P. Duan, *CrystEngComm*, 2013, **15**, 5412; (*b*) L. S. Long, *CrystEngComm*, 2010, **12**, 1354; (*c*) C. P. Li, Q. Yu, J. Chen and M. Du, *Cryst. Growth Des.*, 2010, **10**, 2650; (*d*) B. Zheng, H. Dong, J. F. Bai, Y. Z. Li, S. H. Li and M. Scheer, *J. Am. Chem. Soc.*, 2008, **130**, 7778.

(12) (*a*) J. Chen, P. W. Liu and C. P. Li, *Inorg. Chem. Commun.*, 2013, **36**, 105; (*b*) M. Du, X. J. Jiang and X. J. Zhao, *Inorg. Chem.*, 2006, **45**, 3998; (*c*) M. Du, Z. H. Zhang and X. J. Zhao, *Inorg. Chem.*, 2006, **45**, 5785.

(13) (*a*) C. P. Li, J. M. Wu and M. Du, *Chem.–Eur. J.*, 2012, **18**, 12437; (*b*) M. Du, C. P. Li, J. M. Wu, J. H. Guo and G. C. Wang, *Chem. Commun.*, 2011, **47**, 8088.

(14) C. P. Li, J. Chen, P. W. Liu and M. Du, *CrystEngComm*, 2013, **15**, 9713.

(15) C. P. Li, J. Chen, P. W. Liu and M. Du, *CrystEngComm*, 2014, **16**, 6433.

(16) A. L. Apek, *J. Appl. Crystallogr.*, 2003, **36**, 7.

(17) Bruker AXS, *SAINT Software Reference Manual*, Madison, WI, 1998.

(18) G. M. Sheldrick, *SHELXTL NT Version 5.1. Program for Solution and Refinement of Crystal Structures*, University of Göttingen, Germany, 1997.

(19) For explanation of the three-letter net codes, see: N. W. Ockwig, O. Delgado-Friedrichs, M. O'Keeffe and O. M. Yaghi, *Acc. Chem. Res.*, 2005, **38**, 176 and the associated web-site http://rcsr.anu.edu.au/.

(20) (*a*) C. Seward, W. L. Jia, R. Y. Wang, G. D. Enright and S. Wang, *Angew. Chem. Int. Ed.*, 2004, **43**, 2933; (*b*) S. L. Zheng, J. H. Yang, X. L. Yu, X. M. Chen and W. T. Wong, *Inorg. Chem.*, 2004, **43**, 830; (*c*) R. H. Wang, L. Han, F. L. Jiang, Y. F. Zhou, D. Q. Yuan and M. C. Hong, *Cryst. Growth Des.*, 2005, **5**, 129.

Caption to Figures

Fig. 1 Crystal structure for **1**. (a) Coordination geometry of Zn(II) (symmetry codes for A = $-x + 1/2, -y + 1/2, z$; B = $-x, -y + 1/2, z + 1/2$; C = $x + 1/2, y, z + 1/2$), with all non-H atoms in ORTEP style at 50% ellipsoid probability. (b) 2D coordination layer with rhombic meshes. (c) Interdigitating arrangement of the parallel 2D layers.

Fig. 2 Crystal structure for **2**. (a) Coordination geometry of Zn(II) (symmetry codes for A = $-x + 1, y, -z + 1/2$; B = $x, -y, z + 1/2$; C = $x - 1/2, -y + 1/2, z - 1/2$), with all non-H atoms in ORTEP style at 50% ellipsoid probability, in which the ligand backbones for 2- and 3-connected L-Cl^- linkers are shown in pink and green, respectively. (b) (left) 3D coordination network and (right) the highlighted 1D chains therein extended by μ_2- and μ_3-L-Cl^- ligands along different directions. (c) Schematic representation of the binodal (3,6)-connected network, in which blue and green nodes represent Zn(II) and L-Cl^-, respectively. (d) Simplified representation of the **dia** net with $[Zn_2(H_2O)(COO)_2]$ SBUs as nodes.

Fig. 3 Crystal structure for **3**. (a) Coordination geometry of Zn(II) (symmetry codes for A = $x + 1, y, z$; B = $x, y - 1, z$), with all non-H atoms in ORTEP style at 50% ellipsoid probability. (b) 2D coordination layer with tetragonal meshes. (c) 3D supramolecular network via O–H···O (red dashed lines) and aromatic stacking interactions (purple dashed lines).

Fig. 4 Crystal structure for **4**. (a) Coordination geometry of Zn(II) (symmetry codes for A = $x + 1/2, y + 1/2, z$; B = $-x + 1/2, y + 1/2, -z + 1/2$; C = $-x + 1, y, -z + 1/2$), with all non-H atoms in ORTEP style at 50% ellipsoid probability. (b) 2D coordination layer with rhombic meshes viewed along the *c* axis. (c) 3D supramolecular network via aromatic stacking interactions (purple dashed lines).

Fig. 5 Crystal structure for **6**. (a) Coordination geometries of Zn(II) (symmetry codes for A = $-x, y, -z + 3/2$; B = $-x, -y, -z + 1$), with all non-H atoms in ORTEP style at 50% ellipsoid probability. (b) 2D supramolecular layer via O–H···O/O–H ···N (red dashed lines), and aromatic stacking interactions (purple dashed lines).

Fig. 6 Solid-state emission spectra for HL-X ligands and complexes **1**–**7**.

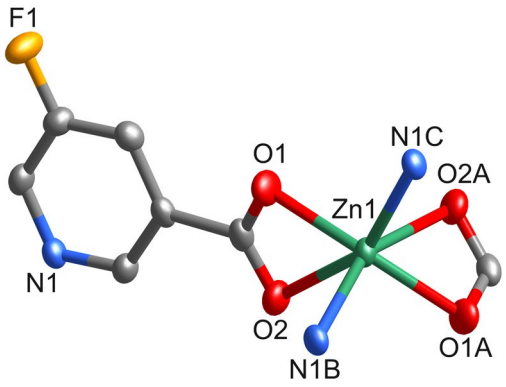

(a)

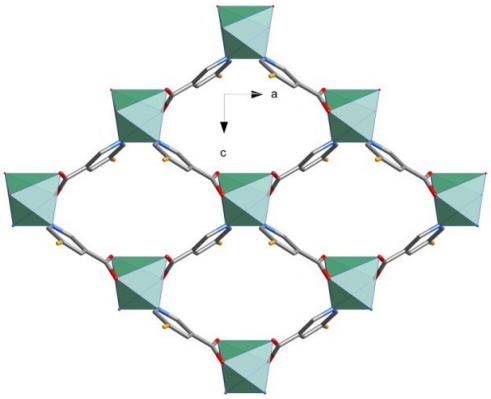

(b)

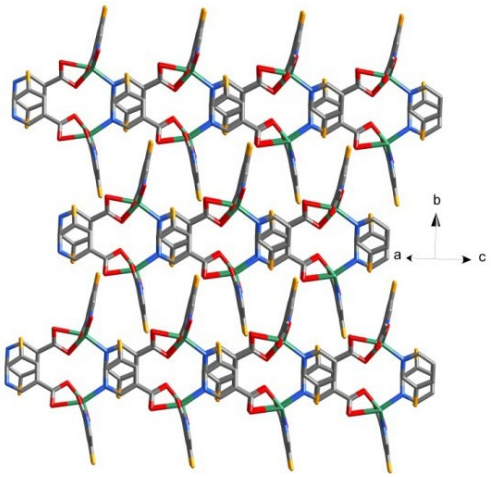

(c)

Fig. 1

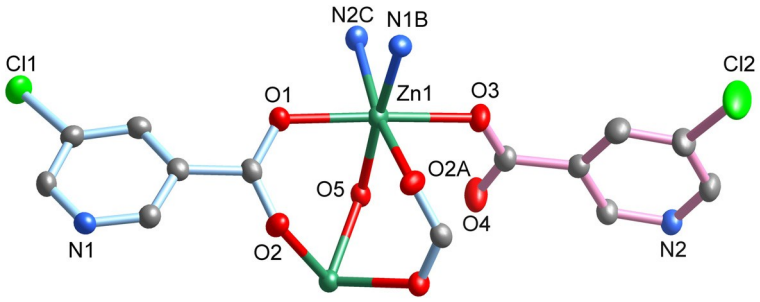

(a)

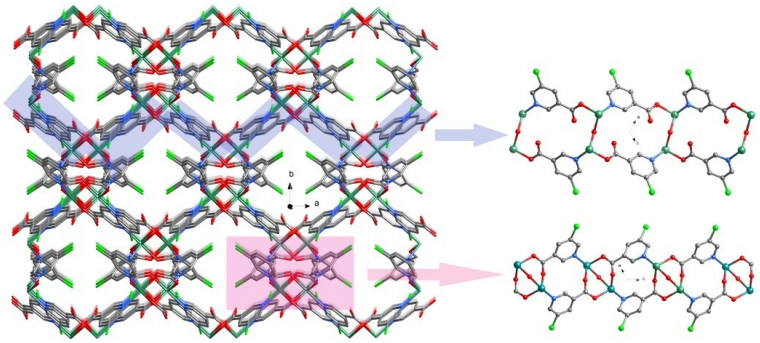

(b)

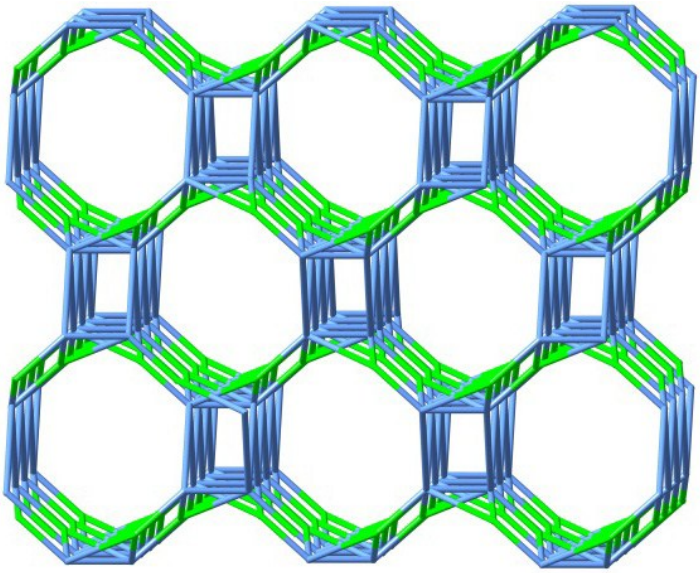

(c)

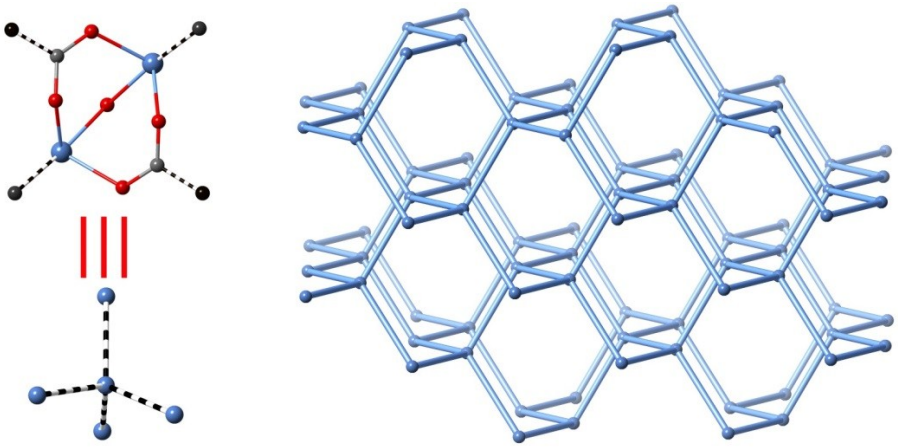

(d)

Fig. 2

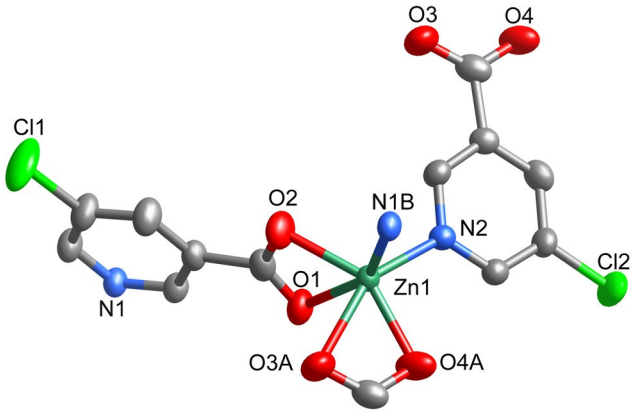

(a)

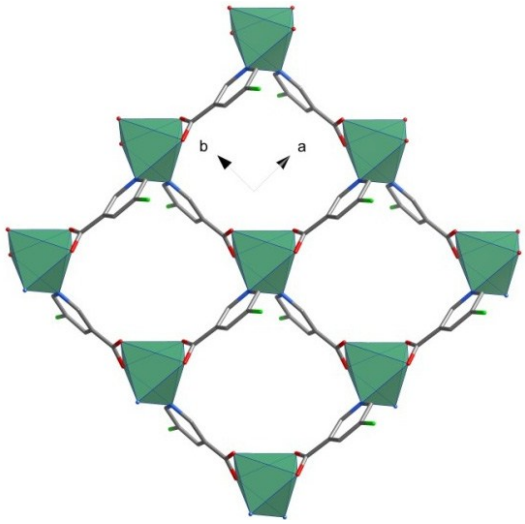

(b)

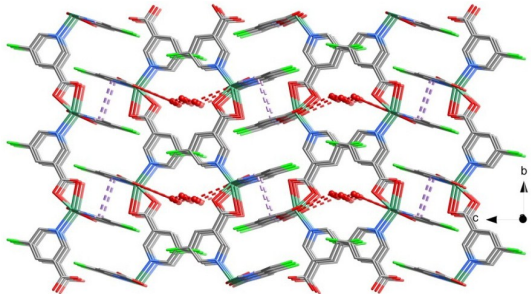

(c)

Fig. 3

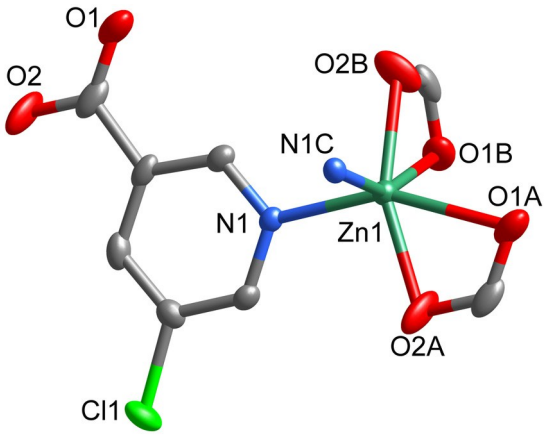

(a)

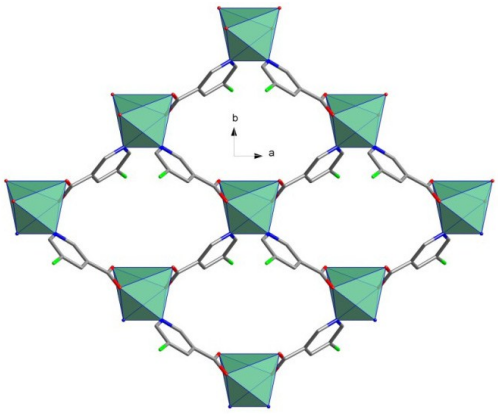

(b)

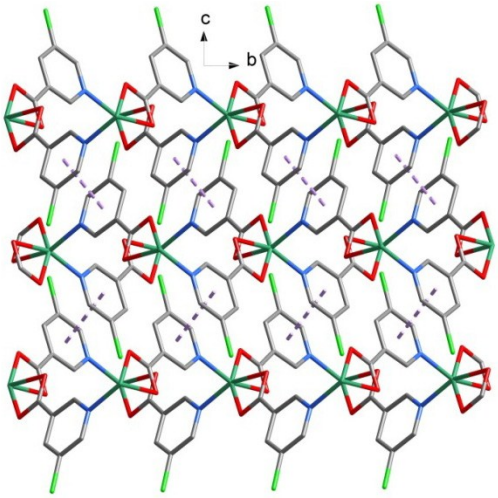

(c)

Fig. 4

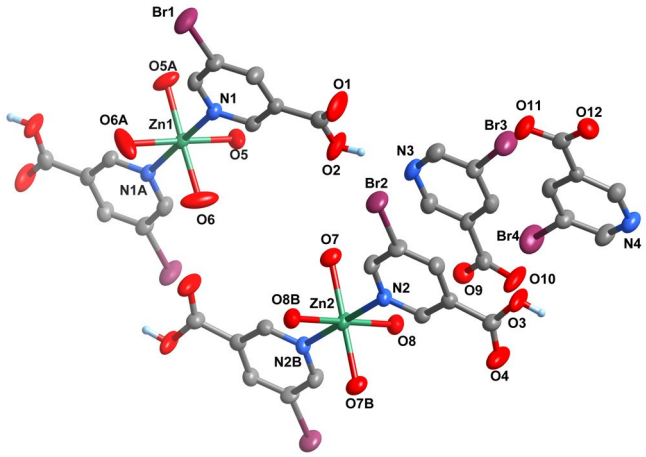

(a)

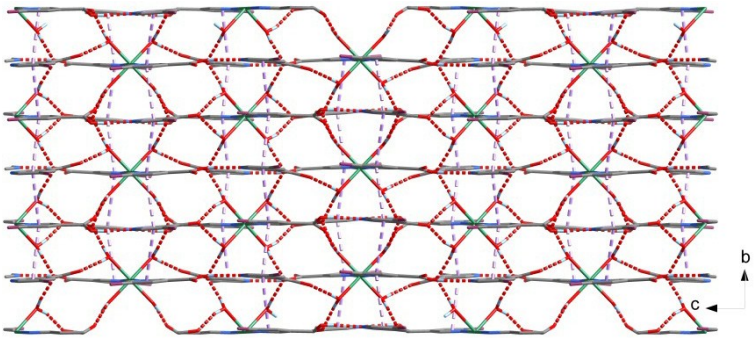

(b)

Fig. 5

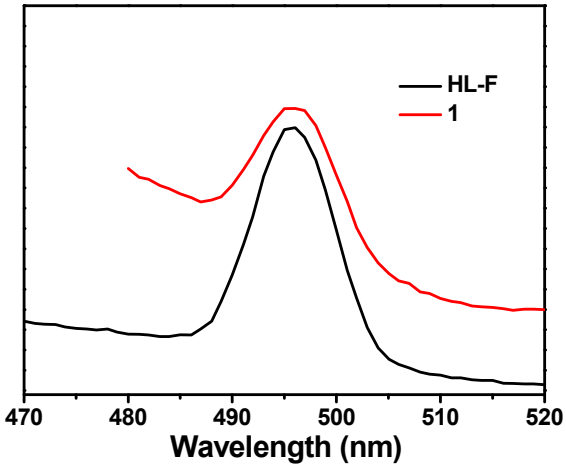

(a)

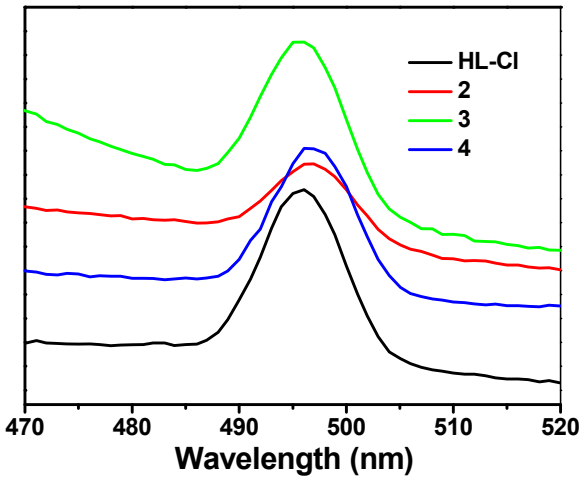

(b)

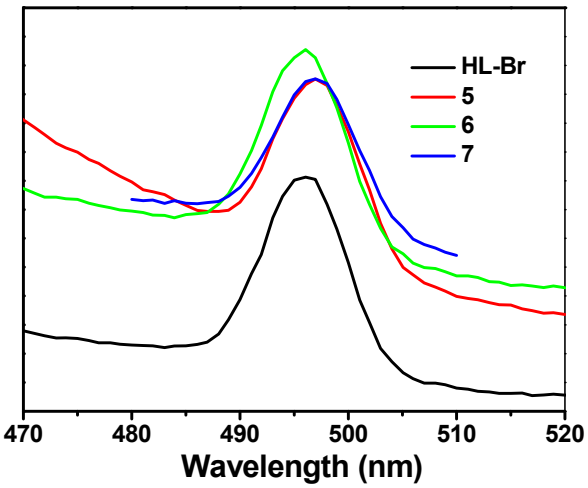

(c)

Fig. 6

Graphical Abstract

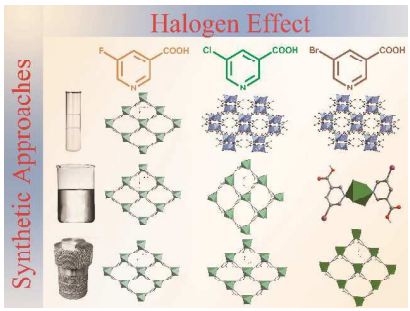

The significant influence of synthetic approach and halogen substituent on Zn(II) coordination assemblies with 5-halonicotinic acids has been demonstrated.